

## SOME THEORETICAL OBSERVATIONS ON CONICAL FAILURE CRITERIA IN PRINCIPAL STRESS SPACE

D. V. GRIFFITHS

University of Manchester, Simon Engineering Laboratories, Oxford Road,  
 Manchester M13 9PL, U.K.

(Received 13 February 1984; in revised form 13 August 1985)

**Abstract**—The properties of the conical failure criteria that lie just inside and just outside the Mohr–Coulomb surface are discussed. Expressions are developed for the maximum stress ratio predicted by these surfaces as a function of the angular stress invariant. For plane strain problems, assuming elastoplastic behaviour, the effect of Poisson’s ratio and the dilation angle on the stress paths and failure loads have been expressed in a closed-form solution. Finally, the expressions are confirmed using finite element analysis of a simple boundary value problem.

### 1. INTRODUCTION

This paper considers some of the properties of conical failure criteria in principal stress space which, in the past, have been postulated as suitable for representing soil strength. The surfaces considered here lie just inside, and just outside, the hexagonal surface of Mohr–Coulomb (Fig. 1). Because the names given to these surfaces by different authors have tended to be somewhat ambiguous, they will be referred to here as the Internal cone and the External cone.

Several authors in the past have considered these surfaces. For example, Bishop[1] showed that the External cone contained a singularity when the friction angle  $\phi$  approached  $36.9^\circ$ , giving an infinite stress ratio in triaxial extension. Zienkiewicz *et al.*[2] implemented several different conical surfaces in a boundary value problem of bearing capacity and computed a wide range of collapse loads. It appeared that subtle changes in the cross-section of a failure surface could have a significant effect.

It is felt that the Mohr–Coulomb failure surface is still the simplest and most appropriate for use in soil mechanics, and it is not the author’s intention to resurrect the use of conical surfaces. It is hoped, however, that the following discussion may improve understanding of the fundamental behaviour of these and other surfaces.

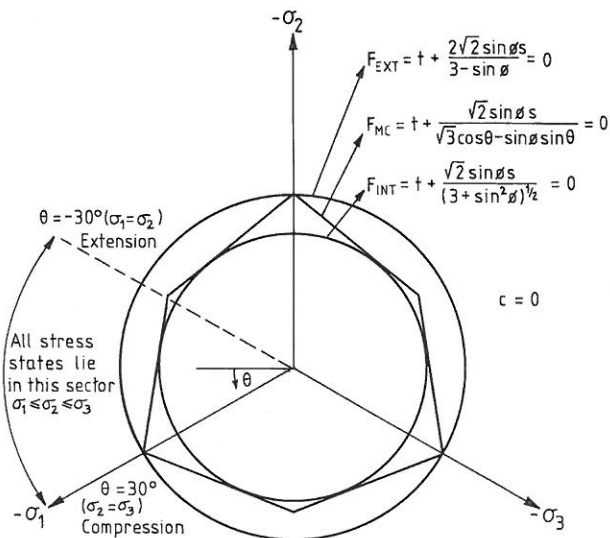


Fig. 1. Conical yield criteria.

## 2. REPRESENTATION OF STRESS IN PRINCIPAL STRESS SPACE

A compression-negative sign convention is assumed throughout, and a stress point in principal stress space is defined using the invariants

$$(s, t, \theta), \quad (1)$$

where

$$s = \frac{1}{\sqrt{3}}(\sigma_x + \sigma_y + \sigma_z) \quad (2)$$

$$t = \frac{1}{\sqrt{3}}[(\sigma_x - \sigma_y)^2 + (\sigma_y - \sigma_z)^2 + (\sigma_z - \sigma_x)^2 + 6\tau_{xy}^2 + 6\tau_{yz}^2 + 6\tau_{zx}^2]^{1/2} \quad (3)$$

and

$$\theta = \frac{1}{3} \arcsin\left(\frac{-3\sqrt{6}J_3}{t^3}\right). \quad (4)$$

The third deviatoric stress invariant is given by

$$J_3 = s_x s_y s_z - s_x \tau_{yz}^2 - s_y \tau_{zx}^2 - s_z \tau_{xy}^2 + 2\tau_{xy} \tau_{yz} \tau_{zx}, \quad (5)$$

where

$$s_x = (2\sigma_x - \sigma_y - \sigma_z)/3, \text{ etc.}$$

In this notation,  $s$  gives the perpendicular distance of the  $\pi$ -plane, from the origin, and  $(t, \theta)$  act as polar coordinates within that plane. Other invariants are equally applicable[3], but those given in expression (1) are favoured by this author because they represent actual lengths in principal stress space.

The principal stresses are easily obtained from the invariants to give

$$\begin{aligned} \sigma_1 &= \frac{s}{\sqrt{3}} + \sqrt{\frac{2}{3}} t \sin\left(\theta - \frac{2\pi}{3}\right), \\ \sigma_2 &= \frac{s}{\sqrt{3}} + \sqrt{\frac{2}{3}} t \sin \theta, \\ \sigma_3 &= \frac{s}{\sqrt{3}} + \sqrt{\frac{2}{3}} t \sin\left(\theta + \frac{2\pi}{3}\right). \end{aligned} \quad (6)$$

Noting that  $\sin(\theta + 2\pi/3) \geq \sin \theta \geq \sin(\theta - 2\pi/3)$ , eqn (6) ensures that  $\sigma_1$  is the smallest of the three principal stresses and hence the most compressive.

The angular invariant  $\theta$  from eqn (4) can be shown to vary in the range  $-30^\circ \leq \theta \leq 30^\circ$ . The lower bound corresponds to a positive principal axis in the  $\pi$ -plane and triaxial extension conditions, whereas the upper bound corresponds to a negative principal axis in the  $\pi$ -plane and triaxial compression conditions. All other stress conditions, such as plane strain for example, correspond to intermediate values of  $\theta$ .

Bishop[1] defined a parameter,  $b$ , which gave the magnitude of  $\sigma_2$  relative to  $\sigma_1$  and  $\sigma_3$ , where

$$b = (\sigma_2 - \sigma_3)/(\sigma_1 - \sigma_3). \quad (7)$$

It follows, then, that the angular invariant is related to Bishop's  $b$  as follows:

$$\theta = \arctan [(1 - 2b)/\sqrt{3}], \quad (8)$$

and hence

$$\sigma_2 = \frac{1}{2}[\sigma_1 + \sigma_3 - \sqrt{3}(\sigma_1 - \sigma_3) \tan \theta]. \quad (9)$$

In the derivations that follow, reference will be made to two measures of shear stress level or strength; the invariant "shear stress level"  $t/s$ , and the "stress ratio"  $\sigma_1/\sigma_3$  with the latter given by the symbol,  $R$ .

These two quantities are related from eqn (6), giving

$$R = \frac{1 + \sqrt{2}(t/s) \sin(\theta - 2\pi/3)}{1 + \sqrt{2}(t/s) \sin(\theta + 2\pi/3)}. \quad (10)$$

### 3. THE FAILURE CRITERIA

#### 3.1. Mohr-Coulomb

In terms of principal stresses, this criterion may be written thus:

$$\frac{\sigma_1 + \sigma_3}{2} \sin \phi - \frac{\sigma_1 - \sigma_3}{2} - c \cos \phi = 0,$$

where  $\phi$  and  $c$  are the familiar friction angle and cohesion of the soil. Substitution of the principal stresses from eqn (6) gives

$$t = \frac{-\sqrt{2} \sin \phi s}{\sqrt{3} \cos \theta - \sin \theta \sin \phi} + \frac{\sqrt{6} \cos \phi c}{\sqrt{3} \cos \theta - \sin \theta \sin \phi}, \quad (11)$$

which, for a cohesionless soil, may be written in terms of the shear stress level at failure, where

$$\left(\frac{t}{s}\right)_f = \frac{-\sqrt{2} \sin \phi}{\sqrt{3} \cos \theta - \sin \theta \sin \phi}. \quad (12)$$

The shear stress level can be thought of as the tangent of the angle of inclination of the failure surface to the space diagonal. In the case of Mohr-Coulomb's criterion, this is a function of the angular stress invariant  $\theta$  as shown in eqn (12).

#### 3.2. External cone

The shear stress level at failure for a conical surface is a constant. For the External cone, it is found by making the substitution  $\theta = 30^\circ$  into eqn (12), as this is the point at which the External cone coincides with Mohr-Coulomb corresponding to triaxial compression stress conditions.

In general,

$$t = \frac{-2\sqrt{2} \sin \phi s}{3 - \sin \phi} + \frac{2\sqrt{6} \cos \phi c}{3 - \sin \phi}, \quad (13)$$

and for a cohesionless soil,

$$\left(\frac{t}{s}\right)_f = \frac{-2\sqrt{2} \sin \phi}{3 - \sin \phi}. \quad (14)$$

### 3.3. Internal cone

This cone is internally tangential to the Mohr–Coulomb surface and is obtained from Mohr–Coulomb's expression by making the substitution[4]

$$\theta = \arctan(-\sin \phi / \sqrt{3}). \quad (15)$$

This leads to the general expression

$$t = \frac{-\sqrt{2} \sin \phi s}{(3 + \sin^2 \phi)^{1/2}} + \frac{\sqrt{6} \cos \phi c}{(3 + \sin^2 \phi)^{1/2}}, \quad (16)$$

which for cohesionless soil becomes

$$\left(\frac{t}{s}\right)_f = \frac{-\sqrt{2} \sin \phi}{(3 + \sin^2 \phi)^{1/2}}. \quad (17)$$

## 4. STRESS RATIO AT FAILURE

The stress ratio of a soil at failure is a commonly used measure of strength in geotechnical engineering, and it is of interest to note the values of  $R_f$  predicted by the three criteria considered above.

### 4.1. Mohr–Coulomb

By definition, the stress ratio at failure is a constant given by

$$R_f = \tan^2(\pi/4 + \phi/2). \quad (18)$$

### 4.2. External cone

Although  $(t/s)_f$  is a constant given by eqn (14), the stress ratio at failure is a function of  $\theta$ .

By substituting eqn (14) into eqn (10), the following expression is obtained:

$$R_f = \frac{3 - \sin \phi - 4 \sin \phi \sin(\theta - 2\pi/3)}{3 - \sin \phi - 4 \sin \phi \sin(\theta + 2\pi/3)}, \quad (19)$$

which becomes singular whenever  $\phi$  and  $\theta$  combine to make the denominator zero. The most important and best known singularity[1] occurs in triaxial extension ( $\theta = -30^\circ$ ) when  $\phi = 36.9^\circ$ . It is interesting to note, however, that for smaller values of  $\phi$ , the maximum stress ratio does not occur at the triaxial extension position, but at an intermediate value of the angular invariant given by the expression

$$dR_f/d\theta = 0. \quad (20)$$

Solution of eqn (20) gives

$$\theta_{\max} = \arcsin[-2 \sin \phi / (3 - \sin \phi)]; \quad (21)$$

hence the maximum stress ratio always occurs at a negative value of the angular stress invariant.

Substitution of  $\theta_{\max}$  into eqn (19) leads to

$$R_{f_{\max}} = \frac{(3 - 2 \sin \phi - \sin^2 \phi)^{1/2} + 2 \sin \phi}{(3 - 2 \sin \phi - \sin^2 \phi)^{1/2} - 2 \sin \phi}. \quad (22)$$

Figure 2(a) shows the variation of eqn (19) for different values of the soil friction

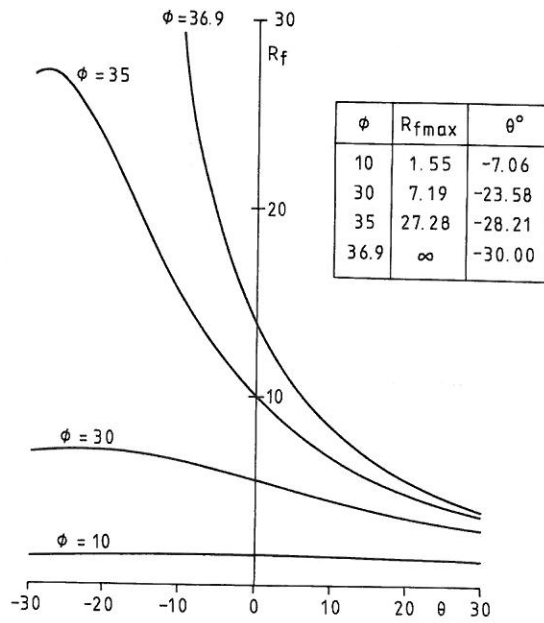


Fig. 2(a). Stress ratio at failure for External cone.

angle. As would be expected, with the exception of triaxial compression conditions ( $\theta = +30^\circ$ ), Mohr-Coulomb's strength is always over-estimated by this surface.

4.3. Internal cone

This surface lies completely within the Mohr-Coulomb surface; hence it will always predict lower strength except at the point where they coincide.

As with the External cone, the stress ratio at failure is a function of  $\theta$ , [Fig. 2(b)], and it can be shown that

$$R_f = \frac{(3 + \sin^2 \phi)^{1/2} - 2 \sin \phi \sin(\theta - 2\pi/3)}{(3 + \sin^2 \phi)^{1/2} - 2 \sin \phi \sin(\theta + 2\pi/3)} \quad (23)$$

with the maximum stress ratio occurring at the tangent point given by eqn (15); hence

$$R_{f\max} = \tan^2(\pi/4 + \phi/2). \quad (24)$$

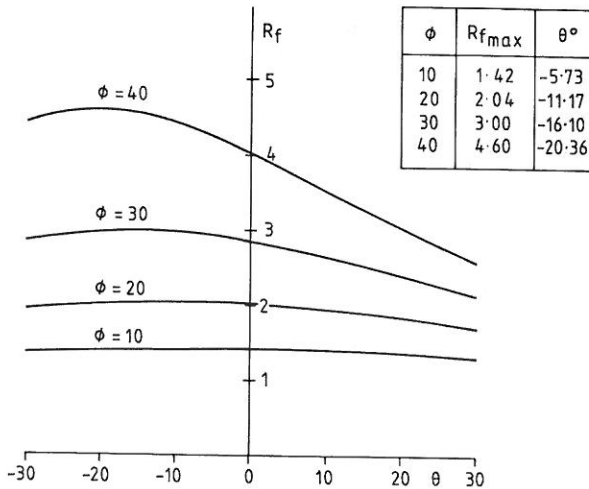


Fig. 2(b). Stress ratio at failure for Internal cone.

## 5. EFFECT OF POISSON'S RATIO

Many problems in soil mechanics deform under plane strain conditions, and for the prediction of collapse loads, elastic-perfectly plastic constitutive models will often be used. Simple models such as these are justified on the grounds that the values of collapse loads are usually insensitive to the soil's constitutive behaviour prior to failure.

A study of the elastic stress paths, however, shows that certain combinations of elastic properties and failure surfaces can affect collapse load predictions[5].

The value of Poisson's ratio is significant in the study of elastic plane strain stress paths. Given that

$$\sigma_2 = \nu(\sigma_1 + \sigma_3), \quad (25)$$

and substituting for  $\sigma_2$  in the principal stress versions of eqns (2) and (3), yield the shear stress level

$$\frac{t}{s} = \frac{-\sqrt{2}(\nu^2 - \nu + 1)^{1/2}}{1 + \nu} \quad (26)$$

and angular stress invariant

$$\theta = \arctan [(1 - 2\nu)/\sqrt{3}]. \quad (27)$$

Equations (26) and (27) show that the plane strain stress path is a function of Poisson's ratio only, and these functions are plotted in Fig. 3. When viewed in a particular  $\pi$ -plane such as that corresponding to  $s = -1$  (Fig. 4), the effect of varying Poisson's ratio between zero and one-half results in a straight line variation. When  $\nu = 0$ , the highest shear stress level is obtained corresponding to triaxial compression ( $\theta = 30^\circ$ ). It may be noted that irrespective of the value of  $\nu$ , the angular stress invariant during elastic deformation is positive.

The fact that the value of Poisson's ratio can influence the shear stress level by up to 73% as it varies between zero and one-half raises the possibility that certain elastic stress paths may not have sufficient inclination to reach a conical surface. This limiting case would occur if the elastic stress path ran parallel to the sides of the cone.

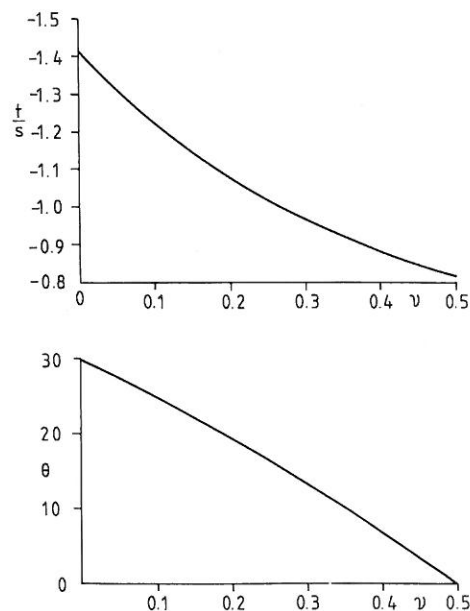


Fig. 3. Stress path for different values of Poisson's ratio in plane strain.

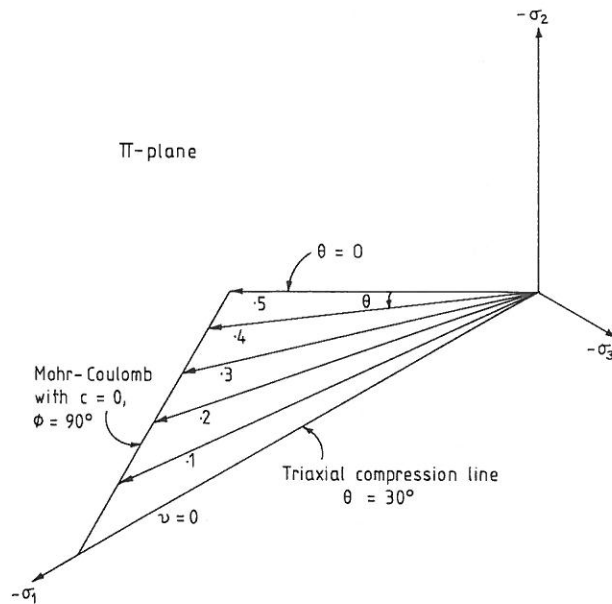


Fig. 4. Effect of Poisson's ratio on plane strain-stress paths in the  $\pi$ -plane.

5.1. Mohr-Coulomb

In the case of the Mohr-Coulomb surface, the shear stress level at failure is a function of the angular invariant  $\theta$ . Substitution of  $t/s$  and  $\theta$  from eqns (26) and (27) into eqn (12) yields the threshold value of  $\phi = 90^\circ$ . This means that for all realistic soil friction angles, the surface will be reached regardless of the value of Poisson's ratio. As shown in Fig. 4, the locus of elastic plane strain stress paths for varying values of Poisson's ratio coincides with the Mohr-Coulomb surface for a friction angle of  $90^\circ$  in the sector defined by  $0 \leq \theta \leq 30^\circ$ .

5.2. External cone

The External cone predicts a stress ratio at failure which varies with  $\theta$  [eqn (19)]. Substitution from eqn (27) given the stress ratio at which the surface is first reached after elastic deformation to be

$$R = \frac{(3 - \sin \phi)(\nu^2 - \nu + 1)^{1/2} - 2(2 - \nu) \sin \phi}{(3 - \sin \phi)(\nu^2 - \nu + 1)^{1/2} - 2(1 + \nu) \sin \phi} \quad (28)$$

As the elastic stress paths can only traverse stress space corresponding to positive values of  $\theta$ , the maximum and minimum values of  $R$  from eqn (28) are given by putting  $\nu = \frac{1}{2}$  and  $\nu = 0$ , respectively, as shown in Fig. 5.

By combining eqns (14) and (26), it is also possible to find the critical combination of friction angle and Poisson's ratio for which the external cone would never be reached by an elastic stress path. This results in eqn (29)

$$\phi = \arcsin \left[ \frac{3(\nu^2 - \nu + 1)^{1/2}}{2(1 + \nu) + (\nu^2 - \nu + 1)^{1/2}} \right] \quad (29)$$

shown plotted in Fig. 6. It is easily shown that eqns (29) and (19) are in fact expressing the same singularity in the external cone. By rearranging eqn (29) and substituting for Poisson's ratio [from eqn (27)], the denominator of eqn (19) (put to zero) can be recovered.

By similar reasoning, the stress ratio at which the Internal cone is first reached in an

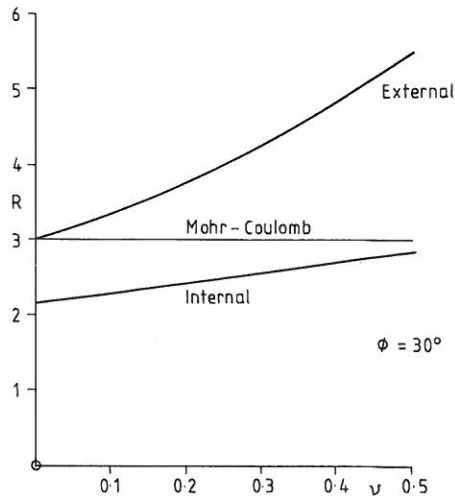


Fig. 5. Stress ratio at "first yield" vs Poisson's ratio in plane strain.

elastic plane strain analysis is given by

$$R = \frac{(3 + \sin^2 \phi)^{1/2}(v^2 - v + 1)^{1/2} + (2 - v) \sin \phi}{(3 + \sin^2 \phi)^{1/2}(v^2 - v + 1)^{1/2} - (1 + v) \sin \phi} \quad (30)$$

As the Internal cone lies wholly within the Mohr-Coulomb surface, it is reached for all values of Poisson's ratio, irrespective of the value of  $\phi$ .

6. ELASTOPLASTIC BEHAVIOUR UNDER PLANE STRAIN CONDITIONS

The previous section was concerned with elastic plane-strain stress paths and showed that the stress ratio  $R$  at which the failure surfaces were first reached could be expressed as a function of Poisson's ratio.

If elastoplastic behaviour in plane strain is considered, however, the ultimate value of the stress ratio predicted by the conical surfaces is always greater than the values given by eqns (28) and (30). This is because the angular invariant of stress,  $\theta$ , changes during plastic straining from its initially positive value during elastic straining to a negative value at failure.

In the following derivations, the potential functions are defined as being algebraically identical to the functions defining the failure surfaces but with  $\phi$  replaced by  $\psi$ . For

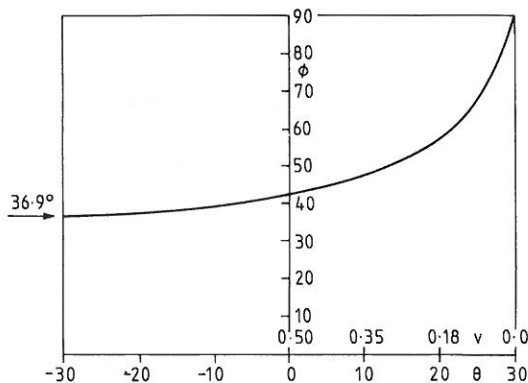


Fig. 6. Limiting  $\phi$  vs Poisson's ratio in plane strain (External cone).



example, if the failure surface is defined as

$$F = 0, \quad (31)$$

then for a cohesionless soil, the External cone from eqn (14) is given by

$$F = t + \frac{2\sqrt{2} \sin \phi}{3 - \sin \phi} s, \quad (32)$$

and the potential function  $Q$  by

$$Q = t + \frac{2\sqrt{2} \sin \psi}{3 - \sin \psi} s. \quad (33)$$

Similarly, for the Internal cone, these functions are defined as

$$F = t + \frac{\sqrt{2} \sin \phi}{(3 + \sin^2 \phi)^{1/2}} s \quad (34)$$

and

$$Q = t + \frac{\sqrt{2} \sin \psi}{(3 + \sin^2 \psi)^{1/2}} s. \quad (35)$$

During plastic yielding, increments of plastic strain are conveniently expressed in terms of volumetric and deviatoric invariants  $\dot{v}^p$  and  $\dot{\gamma}^p$ . These equations are directly analogous to the stress invariants  $s$  and  $t$  [eqns (2) and (3)] with stress components replaced by plastic strain increment components. Plasticity theory states that plastic strain increment directions lie normal to the plastic potential surface  $Q$ , thus during yielding

$$t/s = -\dot{v}^p/\dot{\gamma}^p. \quad (36)$$

Analogous to the stress ratio  $R$  is the "dilatancy rate"  $D$  which is defined as

$$D = 1 - \sqrt{3}(\dot{v}^p/\dot{\epsilon}_1^p), \quad (37)$$

where  $\dot{\epsilon}_1^p$  is the plastic major principal strain increment on an element of material under triaxial or plane strain conditions. According to stress-dilatancy theory[6],  $D$  reaches a maximum at the failure stress ratio. Although  $R$  and  $D$  are not invariants and are only strictly applicable to element tests, the properties they represent are frequently extrapolated to more general loading cases. The remainder of this section, however, will be confined to a discussion of element loading.

At failure, the value of  $D$  given by eqn (37) can be simplified as follows:

$$D = -2\dot{\epsilon}_3^p/\dot{\epsilon}_1^p \quad (\text{triaxial } \dot{\epsilon}_2^p = \dot{\epsilon}_3^p), \quad (38a)$$

$$D = -\dot{\epsilon}_3^p/\dot{\epsilon}_1^p \quad (\text{plane strain } \dot{\epsilon}_2^p = 0). \quad (38b)$$

Furthermore, the plastic strain increment invariants in plane strain at failure are given by

$$\dot{v}^p = \frac{1}{\sqrt{3}} (\dot{\epsilon}_1^p + \dot{\epsilon}_3^p), \quad (39)$$

$$\dot{\gamma}^p = \sqrt{\frac{2}{3}} (\dot{\epsilon}_1^p{}^2 - \dot{\epsilon}_1^p \dot{\epsilon}_3^p + \dot{\epsilon}_3^p{}^2). \quad (40)$$

For Mohr–Coulomb potentials from eqn (12), the invariant dilatancy ratio is given by

$$\frac{\dot{\nu}^p}{\dot{\gamma}^p} = \frac{\sqrt{2} \sin \psi}{\sqrt{3} \cos \theta - \sin \theta \sin \psi}, \quad (41)$$

which from eqns (38b), (39) and (40) can be rearranged as follows:

$$D = \tan^2(\pi/4 + \psi/2). \quad (42)$$

The dilatancy rate in a Mohr–Coulomb material, like the stress ratio, is therefore not dependent upon the value of the angular stress invariant.

For the External cone from eqn (14),

$$\frac{\dot{\nu}^p}{\dot{\gamma}^p} = \frac{2\sqrt{2} \sin \psi}{3 - \sin \psi}; \quad (43)$$

hence

$$D = \frac{3 - \sin \psi - 4 \sin \psi \sin(\theta - 2\pi/3)}{3 - \sin \psi - 4 \sin \psi \sin(\theta + 2\pi/3)}. \quad (44)$$

If at failure,  $D$  is maximised; this occurs when

$$\theta = \arcsin[-2 \sin \psi / (3 - \sin \psi)], \quad (45)$$

and is given by

$$D_{\max} = \frac{(3 - 2 \sin \psi - \sin^2 \psi)^{1/2} + 2 \sin \psi}{(3 - 2 \sin \psi - \sin^2 \psi)^{1/2} - 2 \sin \psi}. \quad (46)$$

The corresponding stress ratio at failure is given by substitution of  $\theta$  from eqn (45) in eqn (19); hence

$$R_f = \frac{3 - \sin \phi - \sin \psi - \sin \phi \sin \psi + 2(3 - 2 \sin \psi - \sin^2 \psi)^{1/2} \sin \phi}{3 - \sin \phi - \sin \psi - \sin \phi \sin \psi - 2(3 - 2 \sin \psi - \sin^2 \psi)^{1/2} \sin \phi}. \quad (47)$$

The stress ratio at failure is thus dependent upon both  $\phi$  and  $\psi$ , as the latter governs the value of the angular invariant to give maximum dilatancy.

Similarly, for the Internal cone from eqn (17),

$$\frac{\dot{\nu}^p}{\dot{\gamma}^p} = \frac{\sqrt{2} \sin \psi}{(3 + \sin^2 \psi)^{1/2}}; \quad (48)$$

hence

$$D = \frac{(3 + \sin^2 \psi)^{1/2} - 2 \sin \psi \sin(\theta - 2\pi/3)}{(3 + \sin^2 \psi)^{1/2} - 2 \sin \psi \sin(\theta + 2\pi/3)}. \quad (49)$$

The maximum dilatancy rate thus occurs when

$$\theta = \arctan(-\sin \psi / \sqrt{3}), \quad (50)$$

giving

$$D_{\max} = \tan^2(\pi/4 + \psi/2). \quad (51)$$

By substitution of  $\theta$  from eqn (50) into eqn (23), the corresponding stress ratio at failure is given by

$$R_f = \frac{2(3 + \sin^2 \phi)^{1/2}(3 + \sin^2 \psi)^{1/2} - 2 \sin \phi \sin \psi + 6 \sin \phi}{2(3 + \sin^2 \phi)^{1/2}(3 + \sin^2 \psi)^{1/2} - 2 \sin \phi \sin \psi - 6 \sin \phi}. \quad (52)$$

It may be noted that the maximum stress ratio that can be achieved for a particular conical failure surface and potential is only possible if using an associated flow rule ( $\psi = \phi$ ). For example, the Internal cone with an associated flow rule will always give strength corresponding to Mohr-Coulomb. This is because eqn (50) gives the value of the angular stress invariant at which the two surfaces coincide. Potts and Gens[7] reached similar conclusions when considering the role of the potential function on plastic deformations under plane strain conditions.

An obvious disadvantage of assuming associated flow is that the dilatancy rate predicted greatly exceeds observed values in the laboratory. Stress dilatancy theory gives that

$$R_f/D_{\max} \simeq 3 \quad (53)$$

for many sand-like materials at failure, whereas associated flow rules with all three surfaces considered here lead to the ratio of eqn (53) equalling unity. It is a fairly simple matter, however, to adjust the dilation angle used in a particular analysis so that eqn (53) is approximately satisfied. This has been done in Fig. 7 for dense materials with  $\phi \geq 30$ .

To test the validity of the previous expressions and the hypothesis that "failure" corresponds to  $D_{\max}$ , an elastoplastic analysis has been performed on a single finite element as shown in Fig. 8. The failure surfaces and potentials were those for the External cone

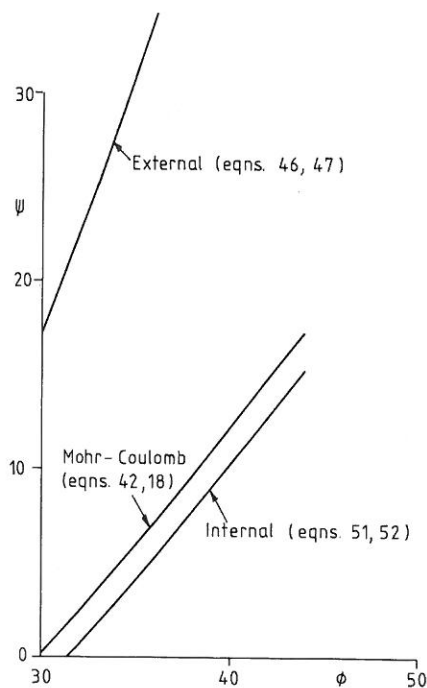


Fig. 7.  $\phi$  vs  $\psi$  to give  $R = 3D$  at failure in plane strain.

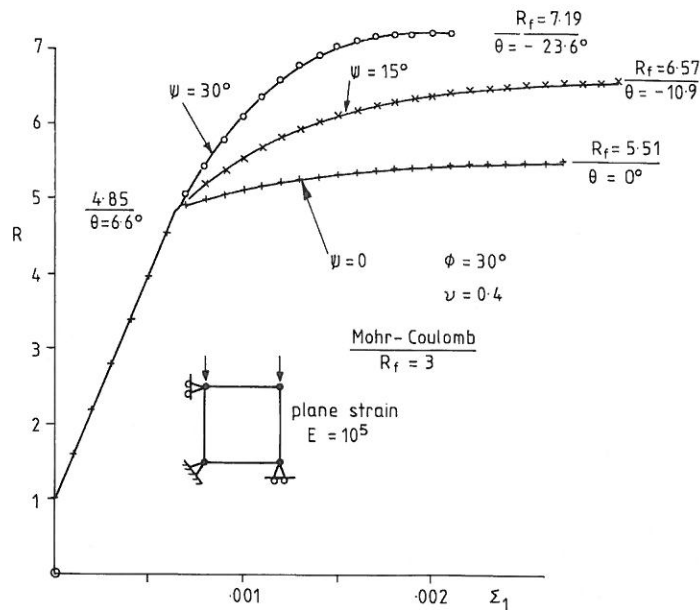


Fig. 8. Stress ratio at failure for different values of the dilation angle (External cone).

and the initial stress state was assumed to be isotropic. For a friction angle of  $30^\circ$  and a Poisson's ratio of 0.4, the analysis was performed with three different dilation angles. Initially, the response is elastic until the failure surface is first reached when  $R = 4.85$  as given by eqn (28). As yielding takes place, the angular stress invariant changes until maximum dilatancy is achieved, and the stress ratio increases to its ultimate value given by eqn (47).

For example, for  $\phi = 30^\circ$  with the External cone, the values of Table 1 are obtained. These values are closely reproduced numerically, as shown in Fig. 8.

It may be noted that when using the external cone, Mohr-Coulomb strengths are considerably overestimated, even when  $\psi = 0$ .

## 7. CONCLUSIONS

The stress path followed by an element of material in an elastoplastic analysis under plane strain conditions has been considered. During the elastic phase, the stress path has been shown to be a function of Poisson's ratio only and can always be predicted provided the initial stress state is known.

For the conical failure surfaces which circumscribe and inscribe the Mohr-Coulomb surface, expressions have been derived giving the maximum ultimate stress ratio that occurs after plastic yielding in plane strain. It is shown that the corresponding ultimate value of the angular invariant of stress is that which corresponds to the maximum rate of plastic dilation. This is uniquely defined by the assumed plastic potential surface and dilation angle. Consequently, provided the functions describing the failure criterion and plastic potential are geometrically similar, maximum strength can only be achieved using an associated flow rule. For the case of the Internal cone, associated flow will always

Table 1. Stress ratio at failure for  $\phi = 30^\circ$   
(External cone)

$\psi$	$\theta$ [eqn (45)]	$R_f$ [eqn (47)]
0	0	5.51
15	-10.9	6.57
30	-23.6	7.19

result in a shear strength identical to that predicted by Mohr–Coulomb. For the External cone, however, even for friction angles less than the well-known singularity at  $\phi = 36.9^\circ$ , the predicted strength considerably overestimates the Mohr–Coulomb value for all values of the dilation angle.

## REFERENCES

1. A. W. Bishop, The strength of soils as engineering materials. 6th Rankine Lecture, *Geotechnique* **16**, 91–130 (1966).
2. O. C. Zienkiewicz, V. A. Norris, L. A. Winnicki, D. J. Naylor and R. W. Lewis, A unified approach to the soil mechanics problems of offshore foundations. *Numerical Methods in Offshore Engineering*, Chap. 12. Wiley, London (1978).
3. G. C. Nayak and O. C. Zienkiewicz, Convenient forms of stress invariants for plasticity. *ASCE, J. Struct. Div.* **98**, 949–954 (1972).
4. D. V. Griffiths, Finite element analyses of walls, footings and slopes. Ph.D. thesis, University of Manchester, pp. 21–26 (1980).
5. A. C. Matos, The numerical influence of Poisson's ratio on the safety factor. *Proc. 4th Int. Conf. Num. Meth. Geomech.* (Edited by Z. Eisenstein), pp. 207–212. Edmonton (1982).
6. P. W. Rowe, Theoretical meaning and observed values of deformation parameters for soil. *Proc. Roscoe Mem. Symp.*, Cambridge, U.K., pp. 548–563 (1971).
7. D. M. Potts and A. Gens, The effect of the plastic potential on boundary value problems involving plane strain deformation. *Int. J. Num. Anal. Meth. Geomech.* **8**, 259–286 (1984).

